

# Topological Bayesian inversion for the inverse conductivity problem

**J. Rocha de Faria**

Departamento de Computação Científica, UFPB  
58051-900, João Pessoa, PB – BRAZIL  
E-mail: jairo@ci.ufpb.br

**D. Lesnic**

Department of Applied Mathematics, University of Leeds  
Leeds, LS2 9JT – UK  
E-mail: amt5ld@maths.leeds.ac.uk.

**Abstract:** *The employment of topological derivative concept is considered to propose a new optimization algorithm for the inverse conductivity problem. Since this inverse problem is nonlinear and ill-posed it is necessary to incorporate a prior knowledge about the unknown conductivity. In particular, we apply the Bayes theorem to add the assumption that we have just one small ball-shaped inclusion, which must be at a certain distance from the boundary of the domain. As the main emphasis of this paper is to investigate numerically the proposed approach, we shall present some numerical results to show that accurate results, even for noisy data, can be obtained with small computational cost.*

**Keywords:** *inverse conductivity problem, topological derivative, Bayesian inversion*

## 1 Introduction

The inverse conductivity problem consists in determining the conductivity distribution of a body from non-intrusive boundary measurements (see [5], Ch.4). This problem sets out a mathematical foundation for the process of electrical impedance tomography (EIT) which is an imaging tool with important applications in fields such as medical diagnosis, nondestructive evaluation of materials, geophysics, land mine detection and other fields; see [1, 2, 3], for example.

An usual way to propose reconstruction algorithms is to recast the inverse geometric problem in the form of a topological optimization problem, taking into account an appropriate shape functional. In particular, the topological derivative, which measures the sensitivity of a given shape functional with respect to an infinitesimal singular domain perturbation, has been recognized as a very useful tool for this analysis [10]. However, in [11] it was shown that the topological derivative in the inverse conductivity problem reaches critical values close to the boundary of the domain. Thus, the classical topological derivative does not provide sufficient information about the inhomogeneity and it is necessary to improve it. An alternative may be to add some prior knowledge on the solution using a Bayesian approach. This framework, denominated Bayesian inversion, is justified by many advantages over deterministic methods, for instance: the variables included in the problem are recognized as random variables which allow an adequate treatment of uncertainties and, the inverse problem is restated as a well-posed extension in a larger space of probability distributions [7, 13].

In this paper, we apply the topological derivative in a Bayesian inversion context and we explore two statistical estimates for the location: the maximum a posteriori estimator and the posterior mean estimator. The first one is analogous to take the classical topological derivative weighted by a function and it leads to a bad estimate. On the other hand, the posterior mean

estimator gives very accurate estimates, even taking into account noisy data. These results, pointed out in the numerical experiments, give the justification for this reason.

## 2 The Inverse Conductivity Problem

We consider a bounded domain  $\Omega \subset \mathbb{R}^2$ , with a connected Lipschitz boundary  $\partial\Omega$ . In addition, we assume that  $\Omega$  contains one small circular inclusion  $B_{r_*}(\mathbf{x}_*)$  of radius  $r_* > 0$ , centered at  $\mathbf{x}_*$  and separated from the boundary  $\partial\Omega$ . More specifically, we have  $B_{r_*}(\mathbf{x}_*) = \mathbf{x}_* + r_*B_1(\mathbf{0})$  and we assume that there exists a constant  $\zeta$  such that  $dist(\partial\Omega, B_{r_*}(\mathbf{x}_*)) > \zeta > 0$ , where  $B_1(\mathbf{0})$  is the unit ball centered at the origin. Further, we assume that the background is homogeneous with unit conductivity and the inhomogeneity  $B_{r_*}(\mathbf{x}_*)$  has a contrast coefficient  $0 < \gamma_* \neq 1 < +\infty$ . Defining  $\Omega_*(\mathbf{x}_*) := \Omega \setminus \overline{B_{r_*}(\mathbf{x}_*)}$ , the conductivity is characterized by the piecewise constant function:  $\gamma(\mathbf{x}) = \chi_{\Omega_*(\mathbf{x}_*)}(\mathbf{x}) + \gamma_*\chi_{B_{r_*}(\mathbf{x}_*)}(\mathbf{x})$ ,  $\mathbf{x} \in \Omega$ , where  $\chi_D$  denotes the characteristic function. The main aim of this work is to develop an algorithm to detect the ball-shaped inclusion  $B_{r_*}(\mathbf{x}_*)$  and the contrast coefficient  $\gamma_*$ .

If we relate to steady-state heat conduction, in order to determine the inclusion, we consider a given non-constant temperature distribution  $\bar{u} \in H^{1/2}(\partial\Omega)$  and measure the boundary heat flux  $0 \neq \bar{q} \in H^{-1/2}(\partial\Omega)$  on the whole boundary  $\partial\Omega$ . The inverse problem considered is to determine the defect  $B_{r_*}(\mathbf{x}_*)$  and the thermal conductivity  $\gamma_*$  from the knowledge of a single pair of Cauchy data  $(\bar{q}, \bar{u})$ . Therefore, we wish to determine  $u_*$ ,  $B_{r_*}(\mathbf{x}_*)$  and  $\gamma_*$  satisfying the following inverse problem:

$$\begin{cases} \nabla \cdot (\gamma \nabla u_*) & = & 0 & \text{in } & \Omega \\ -(\gamma \nabla u_*) \cdot \mathbf{n} & = & \bar{q} & \text{on } & \partial\Omega \\ u_* & = & \bar{u} & \text{on } & \partial\Omega \\ \llbracket u_* \rrbracket & = & 0 & \text{on } & \partial B_{r_*}(\mathbf{x}_*) \\ \llbracket (\gamma \nabla u_*) \rrbracket \cdot \mathbf{n} & = & 0 & \text{on } & \partial B_{r_*}(\mathbf{x}_*) \end{cases}, \tag{1}$$

where the operator  $\llbracket \cdot \rrbracket$  denotes the jump on the boundary of inclusion  $\partial B_{r_*}(\mathbf{x}_*)$  and  $\mathbf{n}$  is the outward unit normal vector. We also assume that the compatibility condition  $\int_{\partial\Omega} \bar{q} = 0$ , is satisfied. The solution to the inverse conductivity problem (1) is unique [6].

### 2.1 The Kohn-Vogelius Functional

Let us consider the background  $\Omega$  perturbed by a small ball-shaped inclusion  $B_\varepsilon(\hat{\mathbf{x}}) = \hat{\mathbf{x}} + \varepsilon B_1(\mathbf{0})$ , with conductivity  $0 < \hat{\gamma} \neq 1 < +\infty$ , size  $\varepsilon > 0$  and centered at an arbitrary point  $\hat{\mathbf{x}} \in \Omega$ , such that  $dist(\partial\Omega, B_\varepsilon(\hat{\mathbf{x}})) > \zeta > 0$ . Define  $\Omega_\varepsilon(\hat{\mathbf{x}}) := \Omega \setminus \overline{B_\varepsilon(\hat{\mathbf{x}})}$ . In this case, the conductivity is characterized by the piecewise constant function  $\gamma_\varepsilon(\mathbf{x}) = \chi_{\Omega_\varepsilon(\hat{\mathbf{x}})}(\mathbf{x}) + \hat{\gamma}\chi_{B_\varepsilon(\hat{\mathbf{x}})}(\mathbf{x})$ ,  $\mathbf{x} \in \Omega$ . The Kohn-Vogelius (KV) functional  $\mathcal{J}_\varepsilon: \Omega \rightarrow \mathbb{R}_+$ , [8], is defined by

$$\mathcal{J}_\varepsilon(\hat{\mathbf{x}}) = \frac{1}{2} \int_{\Omega} \gamma_\varepsilon |\nabla(u_\varepsilon^D - u_\varepsilon^N)|^2, \quad \hat{\mathbf{x}} \in \Omega, \tag{2}$$

where  $u_\varepsilon^D$  and  $u_\varepsilon^N$  are, respectively, the solution of the problems associated to the Dirichlet  $\bar{u}$  and to the Neumann  $\bar{q}$  boundary data, given by:

$$\left\{ \begin{array}{l} \text{Find } u_\varepsilon^D \text{ such that} \\ \nabla \cdot (\gamma_\varepsilon \nabla u_\varepsilon^D) = 0 \quad \text{in } \Omega \\ u_\varepsilon^D = \bar{u} \quad \text{on } \partial\Omega \\ \llbracket u_\varepsilon^D \rrbracket = 0 \quad \text{on } \partial B_\varepsilon(\hat{\mathbf{x}}) \\ \llbracket (\gamma_\varepsilon \nabla u_\varepsilon^D) \rrbracket \cdot \mathbf{n} = 0 \quad \text{on } \partial B_\varepsilon(\hat{\mathbf{x}}) \end{array} \right\}, \quad \left\{ \begin{array}{l} \text{Find } u_\varepsilon^N \text{ such that} \\ \nabla \cdot (\gamma_\varepsilon \nabla u_\varepsilon^N) = 0 \quad \text{in } \Omega \\ -(\gamma_\varepsilon \nabla u_\varepsilon^N) \cdot \mathbf{n} = \bar{q} \quad \text{on } \partial\Omega \\ \llbracket u_\varepsilon^N \rrbracket = 0 \quad \text{on } \partial B_\varepsilon(\hat{\mathbf{x}}) \\ \llbracket (\gamma_\varepsilon \nabla u_\varepsilon^N) \rrbracket \cdot \mathbf{n} = 0 \quad \text{on } \partial B_\varepsilon(\hat{\mathbf{x}}) \\ \int_{\partial\Omega} u_\varepsilon^N = \int_{\partial\Omega} u_\varepsilon^D \end{array} \right\}, \tag{3}$$

where the last normalization condition is added in order to obtain a unique solution to the Neumann problem. Summarising, in order to retrieve the inclusion  $B_{r_*}(\mathbf{x}_*)$  and the coefficient  $\gamma_*$ , we minimize the KV functional (2) by considering the ‘nucleation’ of a circular inclusion  $B_\varepsilon(\hat{\mathbf{x}})$  of conductivity  $\hat{\gamma}$  centered at an arbitrary point  $\hat{\mathbf{x}} \in \Omega$ . A method for taking this into account is the topological derivative concept which is described in the next section.

### 3 Topological Derivative

The topological derivative introduced in [12] is defined as the first-order correction of the asymptotic expansion of a shape functional depending on the domain, with respect to an infinitesimal singular perturbation. This concept has been successfully applied to a large variety of problems, like topological optimization, inverse problems and image processing, an account of which may be found in the recent monograph by Novotny and Sokolowski [10].

Let us consider  $\Omega$  and  $B_\varepsilon(\hat{\mathbf{x}})$  as previously defined, a given shape functional  $\psi(\Omega)$  defined on the background  $\Omega$  and the corresponding functional  $\psi_\varepsilon(\hat{\mathbf{x}})$  defined on the perturbed domain  $\Omega_\varepsilon(\hat{\mathbf{x}})$ . If, for  $\varepsilon$  small enough, the topological asymptotic expansion  $\psi_\varepsilon(\hat{\mathbf{x}}) = \psi(\Omega) + f(\varepsilon)\mathfrak{D}(\hat{\mathbf{x}}) + o(f(\varepsilon))$ , exists, with  $f(\varepsilon) > 0$ ,  $f(\varepsilon) \rightarrow 0$  and  $o(f(\varepsilon))/f(\varepsilon) \rightarrow 0$  as  $\varepsilon \rightarrow 0$ , then  $\mathfrak{D}(\hat{\mathbf{x}})$  is called the topological derivative of  $\psi$  in  $\hat{\mathbf{x}}$ . One of the most remarkable facts about the topological derivative is that it only depends on the solution of problems defined on the unperturbed domain  $\Omega$ . Then, once the direct problems (4) below have been solved, the topological derivative provides an extremely low computational cost initial guess for the minimization of the functional  $\psi_\varepsilon$ . In particular, for the KV functional (2), we have:  $\psi_\varepsilon(\hat{\mathbf{x}}) := \mathcal{J}_\varepsilon(\hat{\mathbf{x}}) = \frac{1}{2} \int_\Omega \gamma_\varepsilon |\nabla(u_\varepsilon^D - u_\varepsilon^N)|^2$  and  $\psi(\Omega) := \mathcal{J}(\Omega) = \frac{1}{2} \int_\Omega |\nabla(u^D - u^N)|^2$ , where  $u^D$  and  $u^N$  are solutions of the Dirichlet and the Neumann problem, respectively:

$$\left\{ \begin{array}{l} \text{Find } u^D \text{ such that} \\ \Delta u^D = 0 \quad \text{in } \Omega \\ u^D = \bar{u} \quad \text{on } \partial\Omega \end{array} \right\}, \quad \left\{ \begin{array}{l} \text{Find } u^N \text{ such that} \\ \Delta u^N = 0 \quad \text{in } \Omega \\ -\nabla u^N \cdot \mathbf{n} = \bar{q} \quad \text{on } \partial\Omega \\ \int_{\partial\Omega} u^N = \int_{\partial\Omega} u^D \end{array} \right\}. \tag{4}$$

In particular, for a planar domain  $\Omega \subset \mathbb{R}^2$ , we have the following result (see [10]).

**Lemma 1.** *For the KV functional and taking into account a circular inclusion, the topological asymptotic expansion is given by*

$$\mathcal{J}_\varepsilon(\hat{\mathbf{x}}) = \mathcal{J}(\Omega) - \pi\varepsilon^2 \frac{1 - \hat{\gamma}}{1 + \hat{\gamma}} \left( |\nabla u^D(\hat{\mathbf{x}})|^2 + |\nabla u^N(\hat{\mathbf{x}})|^2 \right) + o(\varepsilon^2). \tag{5}$$

### 4 Bayesian Approach to Inverse Problems

The fundamental idea behind Bayesian inference is the Bayes’ formula, which is a simple consequence of Kolmogorov axioms for conditional probabilities, given by  $p_{\mathbf{X}|\mathbf{Y}}(\mathbf{x}|\mathbf{y}) \propto p_{\mathbf{Y}|\mathbf{X}}(\mathbf{y}|\mathbf{x})p_{\mathbf{X}}(\mathbf{x})$ , where  $\mathbf{X} \in \mathbb{R}^n$  and  $\mathbf{Y} \in \mathbb{R}^m$  denote the unknown random variable and the corresponding data, respectively;  $p_{\mathbf{X}|\mathbf{Y}}(\mathbf{x}|\mathbf{y})$  is the posterior probability density function (PPDF) of  $\mathbf{X}$  given the data  $\mathbf{y}$ ;  $p_{\mathbf{X}}(\mathbf{x})$  is the prior density function and  $p_{\mathbf{Y}|\mathbf{X}}(\mathbf{y}|\mathbf{x})$  is the likelihood function, which describes the interrelation between the observation and the unknown. We can observe that the Bayesian statistical inference method represents a solution to an inverse problem as a probability distribution of unknown quantities conditional on available data. In fact, it is a remarkable difference between this approach and the deterministic one, which provides only a point estimate. Then, given the posterior distribution, we can calculate different point estimates and spread or interval

estimates. In particular, in this work, we compare two of the most popular statistical estimates: the maximum a posteriori estimator  $\mathbf{x}_{map} = \arg \max_{\mathbf{x}} p_{\mathbf{X}|\mathbf{Y}}(\mathbf{x}|\mathbf{y})$ , and the posterior mean estimator  $\mathbf{x}_{pm} = \mathbf{E}_{\mathbf{X}|\mathbf{Y}}(\mathbf{x}|\mathbf{y})$ , for the centre of the inclusion, where  $\mathbf{E}$  denotes the expectation.

In the following, the centre, size and conductivity of the inclusion are modeled as random variables. From the formula (5), the size and conductivity can be seen as a scale factor to the topological derivative. Then, let  $\mathbf{X}$  be the unknown centre of the inclusion. Taking a Cauchy pair data  $\mathbf{Y} = (\bar{q}, \bar{u})$  we propose the following heuristic construction of the likelihood function, based on the topological derivative of the KV functional:  $p_{\mathbf{Y}|\mathbf{X}}((\bar{q}, \bar{u})|\mathbf{x}) = |\nabla u^D(\hat{\mathbf{x}})|^2 + |\nabla u^N(\hat{\mathbf{x}})|^2$ . This approach gives a new interpretation for the topological derivative: the regions in the interior of the domain where the topological derivative attains minimum values are the regions where it is most likely to find the inclusion. For the prior density we consider, based on the Gaussian densities, the most commonly used for inverse problems,  $p_{1\mathbf{X}}(\mathbf{x}) = \frac{1}{\beta_1} \exp\left(-\frac{|\mathbf{x}|^2}{2\beta_2}\right)$ , where  $\beta_1$ , is a normalizing constant and  $\beta_2$ , is a parameter to be calibrated on a standard example. The motivation for this choice is based on penalizing the topological derivative values near the boundary of the domain and the previous knowledge that there is just one inclusion buried in the domain. From equation (5), we can observe that the size and the conductivity are dependent variables in the topological asymptotic expansion. Then, it is not possible to simultaneously identify both  $r_*$  and  $\gamma_*$  by the topological derivative approach in a deterministic framework. Nevertheless, the Bayesian inversion can provide a joint probability distribution for these parameters. Denoting the estimated centre by  $\mathbf{x}_{est}$ , we consider the following two cases.

**Case 1:** In the first case, the size  $r_*$  is known and the problem is to retrieve  $\gamma_*$  and  $\mathbf{x}_*$ . Then, considering  $\mathbf{X}$  to be the unknown conductivity  $\gamma$  and  $\mathbf{Y} = (r_*, \mathbf{x}_{est})$ , we adopt the following likelihood function  $p_{\mathbf{Y}|\mathbf{X}}((r_*, \mathbf{x}_{est})|\gamma) = \frac{1}{\beta_5} \exp\left(-\frac{|q_{calculated}-\bar{q}|^2}{2\beta_7}\right)$ .

**Case 2:** In the second case,  $\gamma_*$  is known and the problem is to reconstruct the ball  $B_{r_*}(\mathbf{x}_*)$ . Then, considering  $\mathbf{X}$  to be the unknown size  $r$  and  $\mathbf{Y} = (\gamma_*, \mathbf{x}_{est})$ , we adopt the following likelihood function  $p_{\mathbf{Y}|\mathbf{X}}((\gamma_*, \mathbf{x}_{est})|r) = \frac{1}{\beta_6} \exp\left(-\frac{|q_{calculated}-\bar{q}|^2}{2\beta_8}\right)$ .

Where are normalizing constants and  $\beta_7, \beta_8$  are parameters to be calibrated on a standard example. In each case, we assume that the prior distribution is uniform within a prescribed interval and take a sample in order to obtain estimates for the target. The sample size should be large enough to be representative, but should not increase the computational cost considerably. Then it is necessary to find a balance between this cost and the efficiency of the method. We finally note that the choices of distributions are based on common sense and practice, but they are not unique.

## 5 Numerical Examples

In this numerical example we consider the original domain  $\Omega = B_1(\mathbf{0})$  containing the circular inclusion  $B_{r_*}(\mathbf{x}_*) = (x_*, y_*) + r_*B_1(\mathbf{0})$ , satisfying  $(x_* + r_* \cos(\theta))^2 + (y_* + r_* \sin(\theta))^2 < 1$  for  $\theta \in [0, 2\pi)$ . The Cauchy data  $(\bar{q}, \bar{u})$  is constructed from a benchmark test example [9], where the inverse problem (1) has an analytical solution; given by

$$u_*(x, y) = \begin{cases} x, & x \in B_{r_*}(\mathbf{x}_*) \\ x - \frac{(1 - \gamma_*)(x - x_*)}{2} \left[ 1 - \frac{r_*^2}{(x - x_*)^2 + (y - y_*)^2} \right], & x \in \Omega_{r_*}(\mathbf{x}_*) \end{cases}. \quad (6)$$

From equation (6), the Dirichlet data  $\bar{u}(\theta)$  follows immediately and the corresponding Neumann flux data can be derived as

$$\bar{q}(\theta) := \frac{\partial u_*}{\partial r}(1, \theta) = x - \frac{x(1 - \gamma_*)}{2} \left[ 1 - \frac{r_*^2}{(x - x_*)^2 + (y - y_*)^2} \right] - \frac{(x - x_*)(1 - \gamma_*)r_*^2 [x(x - x_*) + y(y - y_*)]}{\left[ (x - x_*)^2 + (y - y_*)^2 \right]^2}, \theta \in [0, 2\pi), \quad (7)$$

where  $x = \cos(\theta)$  and  $y = \sin(\theta)$ . We consider now some noisy perturbation of the data obtained by defining  $\delta = 1.01$  and modifying  $r_* \approx r_*\delta$ ,  $x_* \approx x_*\delta$ ,  $y_* \approx y_*\delta$  and  $\gamma_* \approx \gamma_*\delta$ . Figure 1(a) shows the PPDF for Gaussian prior with  $\beta_2 = 0.3$  for this noisy data. It can be noted that the maximum a posteriori estimator is not a good estimator in this case, as suggested by the asymmetry of the distribution, even though the inclusion is in a region of high likelihood. Table 1 shows some estimates  $x_{pm}$  and  $x_{map}$  for the centre of the inclusion  $(x_*, y_*)$  considering known the size  $r_*\delta$  and the conductivity  $\gamma_*\delta$  perturbed by the noise  $\delta = 1.01$ . The results presented in Table 1 justify the present interpretation of topological derivative in the context of Bayesian inference. In fact, the maximum a posteriori estimator  $x_{map}$  corresponds to taking the topological derivative weighted by a function chosen appropriately, whilst the posterior mean estimator  $x_{pm}$  is a statistical estimator very suitable for the problem under consideration. **Case 1:** Considering that the size of the inclusion is known as  $r_*\delta$  and the estimate for the centre  $(x_*, y_*)$  is given by  $x_{pm}$  shown in Table 1, let us now obtain an estimate for  $\gamma_*$ , taking into account the exact values  $\gamma_* \in \{0.5, 5.0, 10, 15, 20\}$ . Table 2 shows the results for  $\gamma_{pm}$  when  $r_* = 0.10$ , the probability distribution of  $\gamma$  is uniform and we consider a 100 - sample. Figure 1(b) shows the probability distribution function of  $\gamma$  for the case of the first row and fifth column in Table 2. **Case 2:** Now, we consider the case when  $\gamma_*$  is known and the estimate for centre is  $x_{pm}$ . Then, taking into account  $\gamma_* = 10$ ,  $r_* \in \{0.1, 0.15, 0.20\}$  and assuming that  $r$  has a uniform probability distribution between 0.4 and 0.24, Table 3 shows the estimate  $r_{pm}$  for  $r_*$ . Figure 1(c) shows the probability distribution function of  $r$  for the case of the first row and third column in Table 3.

## 6 Conclusions

In this study the topological derivative was employed to build a likelihood function for the inverse conductivity problem in a Bayesian approach, where a new interpretation of the topological derivative allowed us to set up a likelihood function. On the other hand, the prior knowledge that the inhomogeneity is inside the domain was applied to choose the prior distribution of probabilities. The topological derivative was applied to determine the centre of inclusion. It was found that the maximum a posteriori estimator is very poor and that this point estimator corresponds to putting a weight on the topological derivative. On the other hand, the posterior mean estimator gave a stable and accurate retrieval of the centre of the ball-shaped inclusion. Finally, the estimation of the centre was used to get an estimation of the conductivity or size, providing again stable and accurate results even for a very small inclusion. It should be stressed that retrieving small inclusions is very important in medical applications in which detection a tumour, whilst is still small in size, is crucial. Furthermore, this approach overcomes the global minimum obtained in [9]. It is important to emphasize that these results were obtained without numerical sampling methods, unlike the results found in the literature of statistical inverse problems, which significantly increase the computational cost. These promising results show that the application of topological derivative in the Bayesian framework should be investigated even further as it can provide at least a good initial guess for other iterative methods.

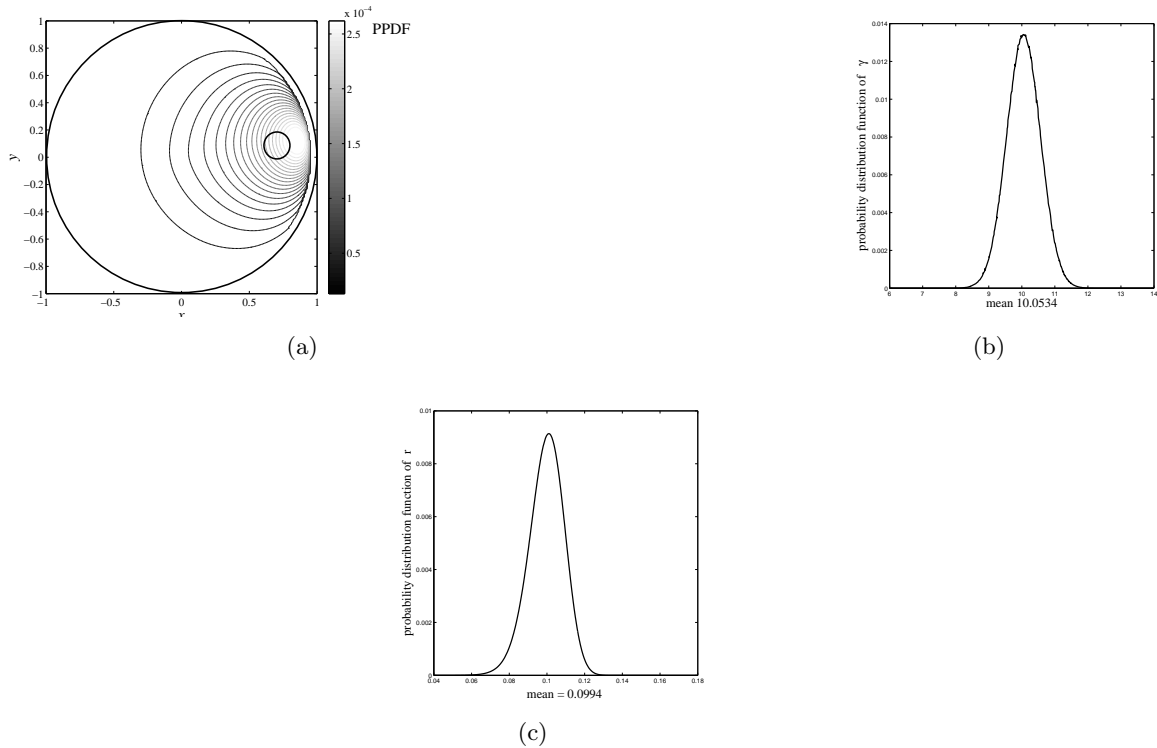


Figure 1: (a) PPDF for Gaussian prior with  $\beta_2 = 0.3$  (b) probability distribution function of  $\gamma$  for the case of the first row and fifth column in Table 2 (c) probability distribution function of  $r$  for the case of the first row and third column in Table 3

<i>Exact</i>	$x_{pm}$	$x_{map}$
$x_* = 0.7$	$x_0 = 0.7152$	$x_0 = 0.8425$
$y_* = 0.1$	$y_0 = 0.1047$	$y_0 = 0.1230$
$r_* = 0.1$		
$\gamma_* = 5.0$		
$x_* = 0.5$	$x_0 = 0.4921$	$x_0 = 0.7020$
$y_* = 0.1$	$y_0 = 0.1004$	$y_0 = 0.1325$
$r_* = 0.2$		
$\gamma_* = 10$		
$x_* = 0.3$	$x_0 = 0.2934$	$x_0 = 0.4250$
$y_* = 0.1$	$y_0 = 0.0943$	$y_0 = 0.1400$
$r_* = 0.2$		
$\gamma_* = 10$		
$x_* = 0.7$	$x_0 = 0.7376$	$x_0 = 0.8015$
$y_* = 0.3$	$y_0 = 0.3185$	$y_0 = 0.3460$
$r_* = 0.1$		
$\gamma_* = 15$		
$x_* = 0.7$	$x_0 = 0.7208$	$x_0 = 0.8435$
$y_* = 0.2$	$y_0 = 0.2039$	$y_0 = 0.2385$
$r_* = 0.1$		
$\gamma_* = 20$		

Table 1: Estimates for the centre of the circular inclusion with noisy data.

## References

- [1] H. Ammari and H. Kang, Reconstruction of Small Inhomogeneities from Boundary Measurements, 429 pages. Springer-Verlag, Berlin (2004)
- [2] L. Borcea, Electrical Impedance Tomography, Inverse Problems, 18, R99–R136 (2002)
- [3] S. Ciulli, M. K. Pidcock and C. Sebu, An Integral Equation Method for the Inverse Conductivity Problem, Physics Letters A, 325, 253–267 (2004)

$(x_*, y_*)$	$x_{pm}$	$\gamma_* = 0.5$	$\gamma_* = 5.0$	$\gamma_* = 10$	$\gamma_* = 15$	$\gamma_* = 20$
		$\gamma_{pm}$	$\gamma_{pm}$	$\gamma_{pm}$	$\gamma_{pm}$	$\gamma_{pm}$
(0.7, 0.1)	(0.7152, 0.1047)	0.5229	5.0423	10.0534	15.0724	19.9360
(0.5, 0.1)	(0.4921, 0.1004)	0.5107	5.0911	10.1296	15.0630	19.9284
(0.3, 0.1)	(0.2934, 0.0943)	0.5143	5.0482	10.1085	15.0817	19.9341
(0.7, 0.3)	(0.7376, 0.3185)	0.4973	5.0693	10.0069	15.0742	19.9518
(0.7, 0.2)	(0.7208, 0.2039)	0.5120	5.0321	10.0393	15.0624	19.9485

Table 2: Estimates for the conductivity  $\gamma_*$  with noisy data.

$(x_*, y_*)$	$x_{pm}$	$r_* = 0.10$	$r_* = 0.15$	$r_* = 0.20$
		$r_{pm}$	$r_{pm}$	$r_{pm}$
(0.7, 0.1)	(0.7152, 0.1047)	0.0994	0.1502	0.1963
(0.5, 0.1)	(0.4921, 0.1004)	0.0974	0.1537	0.2007
(0.3, 0.1)	(0.2934, 0.0943)	0.1003	0.1504	0.2037
(0.7, 0.3)	(0.7376, 0.3185)	0.1002	0.1494	0.2100
(0.7, 0.2)	(0.7208, 0.2039)	0.1008	0.1498	0.2011

Table 3: Estimates for the radius  $r_*$  with noisy data.

- [4] M. Hintermüller and A. Laurain, Electrical Impedance Tomography: From Topology to Shape, *Control Cybern.*, 37(4), 913–933 (2008)
- [5] V. Isakov, *Inverse Problems for Partial Differential Equations*, 284 pages. Springer, New York, (1998)
- [6] V. Isakov and J. Powell, On Inverse Conductivity Problem with One Measurement, *Inverse Problems*, 6, 311–318 (1990)
- [7] J. Kaipio and E. Somersalo, *Statistical and Computational Inverse Problems*, 339 pages. Springer, New York (2005)
- [8] R. Kohn and M. Vogelius, Relaxation of a Variational Method for Impedance Computed Tomography, *Comm. Pure Appl. Math.*, 40(6), 745–777 (1987)
- [9] D. Lesnic, A Numerical Investigation of the Inverse Potential Conductivity Problem in a Circular Inclusion, *Inverse Problems Eng.*, 9, 1–17 (2001)
- [10] A. A. Novotny and J. Sokołowski, *Topological Derivatives in Shape Optimization*, 412 pages. Springer, Berlin (2012)
- [11] J. Rocha de Faria, A. A. Novotny, R. A. Feijóo and E. Taroco, First- and Second-Order Topological Sensitivity Analysis for Inclusions, *Inverse Problems Sci. Eng.*, 17, 665–679 (2009)
- [12] J. Sokołowski and A. Zochowski, On the Topological Derivative in Shape Optimization, *SIAM J. Control Optim.*, 37, 1251–1272 (1999)
- [13] J. Wang and N. Zabaras, Hierarchical Bayesian Models for Inverse Problems in Heat Conduction, *Inverse Problems*, 21, 185–206 (2005)